





CAD Design of Two-stage Cyclone Separator Based on Electronic Information Parameterized Calculation

Zhenhua Han¹  and Mohammad Asif Ikbal² 

¹Zibo Vocational Institute, School of Electronic and Electrical Engineering, Zibo, 255000, China, zhenhuahan8@hotmail.com

²School of Electronics and Electrical Engineering, Lovely Professional University, Punjab, India, asif.22797@lpu.co.in

Corresponding author: Mohammad Asif Ikbal, asif.22797@lpu.co.in

Abstract. Cyclone separator is a kind of equipment used for gas-solid system or liquid-solid system separation. In view of the problems encountered in the repetitive calculation of the cyclone separator and the drawing of parts. The components encountered in the production of enterprises and factories, that is, the problems of more repetitive work and low work efficiency, it is developed based on VB and AutoCAD software. A set of parameterized design software system for the two-stage cyclone separator is considered. Take the inclination angle of the tapered pipe section, the exhaust pipe insertion depth S and the exhaust pipe diameter D , which have a significant effect on the separation efficiency. For design variables, with separation efficiency and pressure drop as objective functions, the structural parameters of the cyclone separator are optimized. The results show that the separation efficiency of the cyclone separator is increased from 84.3% to 90.4% by the response surface optimization method, and the speed, pressure drop, fractionation efficiency before and after optimization are compared and analyzed, and the optimization efficiency is found to be obvious.

Keywords: Cyclone separator; VB and AutoCAD software; Exhaust pipe; Optimization.

DOI: <https://doi.org/10.14733/cadaps.2022.S2.39-51>

1 INTRODUCTION

The cyclone separator is the preferred separation equipment in the field of gas-solid separation. Because it has no moving parts, the maintenance is small, and the pressure drop is not high. Its characteristics are: the greater the flow rate (before a certain value), the higher the separation efficiency. The greater the concentration of the separated solids, the smaller the pressure drop. The cyclone separator has been widely used in the discharge control and product recovery of solid materials with an average particle size of 10 μ m, which can effectively remove particles of various

sizes in dust-containing gases. The main reason hindering the use of cyclone separators to trap fine particles is economic considerations. When a small diameter cyclone separator is used to capture 5 μ m particles, the separation efficiency can reach 90%, but it is not an economical design solution.

The application of cyclone separators is very wide: in the catalytic cracking process, it is the cyclone separator that makes the catalyst. In the operation process, this can be reused by separating and increasing the recovery rate; in combustion and metallurgical plants. It is considered to be at the forefront of environmental protection. At the same time, they are also key components of many internal combustion engines and other air intakes [1]. Therefore, it is necessary to improve and improve the crushing operation. In order to reasonably select the crushing process and improve the grinding machinery, which is of great significance to improve the quality and quantity of products by reducing the power consumption and production cost. Therefore, this operation is important in order to achieve high quality, high yield and low consumption [2]. CAD is a new technology formed by the combination of computer science and engineering design. It is one of the most influential application technologies of computer in engineering. It is also an important part of advanced manufacturing technology [3].

There are many shortcomings in the practical application of two-dimensional drawing in design analysis, which cannot be recognized by the new finite element analysis software [4]. However, when using the finite element software to carry out the finite element modeling analysis, it is necessary to reconstruct the three-dimensional model to make the product more visual, which leads to the lengthening of the development cycle [5]. As an important part of many mechanical products, screw has a wide range of applications in the mechanical field. Because of the different forming mechanism of the spiral surface profile of different screws and the complicated and changeable profile, the processing of the screw is becoming more and more difficult [6].

Computer-aided design and manufacturing (CADD/CAM) technology is the basis of digital and information manufacturing technology [7], and has a wide range of applications in screw design and manufacturing. Scholars have done a lot of research on screw CADD/CAM technology. Authors have developed the parametric design system of the two-dimensional parts drawing of the extrusion screw by using the SolidWorks secondary development principle based on the Visual Basic 6.0 environment and the method of transferring screw parameters through the Access database [8]. In other reported work authors have uses UG as the development platform and Visual C++ 6.0 as the programming tool.

The rest of the manuscript is organized as the most recent work carried out in the design of two stage cyclone operator including artificial intelligent method and the Feature parameterization method is described in Section 2. Section 3 present the experimental setup which is followed by the results and analysis in Section 4. At last, the conclusion drawn from the research is described in Section 5.

2 LITERATURE REVIEW

The product models constructed by the original CAD system are all simple combinations of collective pixels (points, lines, circles, etc.). It is difficult to modify the model and generate new designs. Parametric design methods are an effective way to solve this problem. . From the perspective of the application of parametric technology in mechanical product design, the development process of parametric technology has roughly gone through the following five stages: two-dimensional CAD stand-alone work; solid modeling technology and three-dimensional system development; parameterization and variable technology; product information Model PDM/ERP integration; integrated development system based on product development platform. In recent years, the secondary development of CAD based on the product platform has been widely used in the field of machinery manufacturing at home and abroad. Foreign Quanfu, Q. U. proposed a modeling method rule to adjust the mapping relationship between geometry and functionality, form the best layout of the product family, and obtain the core platform of the product [9].

Chen creates a kind of quantitatively describe the core platform of the relationship between product diversity and parts sharing [10]. Yuqin, Y. proposed a design idea of variable parameter platform [11]. Wang, L. established the core structure of serialized products based on reasoning rules and graphical representation methods [12]. Many domestic scholars have also carried out related research. For example, Wang Aimin and others established a product modular family method based on structural design matrix; Liu Fang adopted a product platform method based on similar functions. It can be seen from the survey that the goal of parametric technology development is to develop an open and extensible design platform, so as to realize the rapid and intelligent design of corresponding products.

The separation mechanism of the cyclone separator is closely related to the critical particle size. The critical diameter d_c (Critical Diameter) refers to the size of the smallest dust particles that can be captured by the cyclone separator. There are two critical particle sizes; d_{c50} and d_{c100} . Particles larger than d_{c50} can be captured by the separator, while particles larger than d_{c100} can be captured by 100%. Since the gas-solid two-phase flow in the separator is very complicated, so far there is no separation theory that can accurately reflect various influencing factors. The current separation theories are based on certain assumptions and are obtained on a simplified basis. The more prominent separation theories are the theory of revolution, equilibrium orbit theory and boundary layer separation theory.

Parametric design is to express design tasks, design goals, design constraints, calculation theories and design results with design variables and a clear and unified model, so as to be modified and realized according to actual design needs in the subsequent human-computer interaction process. The main methods of technical parametric design are:

2.1 Artificial Intelligence Method

This is a new type of expert knowledge system, which can solve the geometric dimensions, positions and constraints in graphics, and use geometric algorithms to derive new geometric constraints. Because geometric features or constraint conditions need to be verified in the inference process, the system built by this method is relatively large and is limited by the hardware performance of the computer.

2.2 Feature Parameterization Method

This type of method first establishes the geometric characteristics of the parameterized model in parameterization, and then combines the feature-based design method with the parameter programming method, so that a variety of different design methods and method.

2.3 Programming-based Parameterization Method

This method determines the geometric relationship between the dimensions of the template and the constraint relationship between the dimensions by analyzing the geometric shape and geometric characteristics of the model, and the application of high-level language or some professional CAD software. The secondary development interface is used to program to realize the size drive, realize the parameterization of the product, and achieve the goal of programmed design. This method is very suitable for occasions where the structural shape does not change much, and only the size changes. It is very suitable for secondary development based on CAD software, to improve and improve the limitations of these general CAD software in professional applications, which is beneficial to the system Targeted development and meet the needs of different users.

This article aims at the repetitive design problems of similar products encountered in the production of enterprises and factories, compiles programs, and uses computers for automated calculation, drawing, assembly and analysis. The design is based on the basic parameters or the parameter table of the database, and completes the calculation of the parameters of each component of the secondary cyclone, such as the area, blanking, geometric size, volume, weight

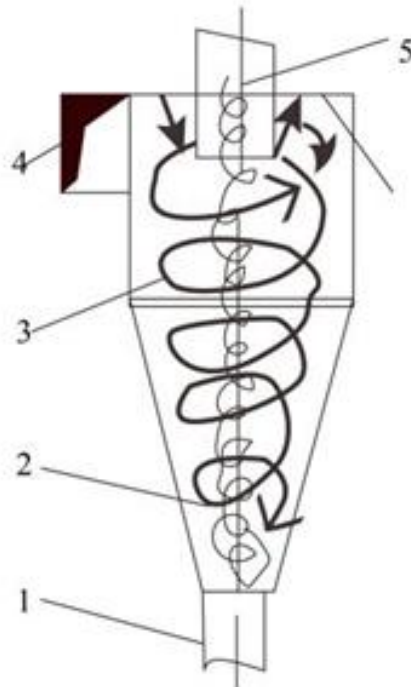
and other parameters of the sheet metal half-radius expansion. Realize the connection between VB and CAD program, complete the parametric realization of engineering drawings, complete the parametric design and programming of the part drawing of the secondary cyclone separator, and the computer automatically draws the part drawing and saves the drawing. Realize the parameterization of three-dimensional parts and assembly, and complete automatic assembly between parts. Perform basic flow field analysis on the internal flow field of the cyclone to investigate and verify the performance of the designed product [13].

3 EXPERIMENT PREPARATION

3.1 Basic Structure and Working Principle of Cyclone Separator

3.1.1 Basic structure of cyclone separator

The basic of the cyclone separator is shown in Figure 1. It is composed of an ash discharge pipe 1, an intake pipe 4, an exhaust pipe 5, a cylinder and a cone separation part. The structure of the cyclone separator can be designed into a variety of styles according to needs, which constitutes different types of cyclone separators, but the size is changed, but the separation principle is the same.



1. Ash pipe 2. Internal swirl flow 4.intake-tube 5. escape-pipe 6. Cyclone roof

Figure 1: Cyclone separator.

3.1.2 Working principle of cyclone separator

The separation principles of the cyclone separator mainly include the "balanced orbit" model, the "dwell time" model, etc. The researchers found through repeated experiments that the Barth model theory in the balanced orbit model accords with the experimental results relatively well. The Barth model extends the overflow pipe to the discharge port of the separator, so that a false CS

surface is formed inside the separator, as shown in Figure 2. After the separated solid-containing gas enters the separation chamber, due to the action of gravity, the solid particles have a downward synthesis speed with the initial velocity when entering the separation chamber. This speed direction is downward, and because the gas enters on the wall of the separation chamber Therefore, a spiral descending line along the wall of the separation chamber is formed. Finally, the solid particles are removed from the ash discharge pipe under the action of gravity, and the separated gas is under pressure from the center of the separation chamber due to its low density. It moves downward and upward and is discharged from the exhaust port to form a separation of gas-solid and phase mixture as shown in Figure 2.

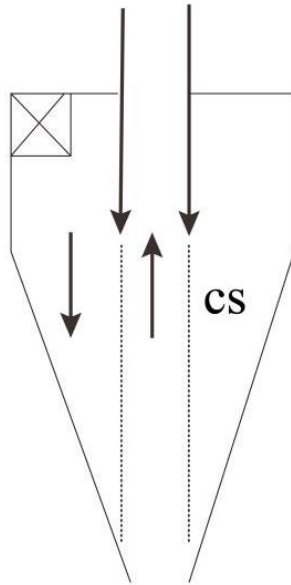


Figure 2: The imaginary CS surface.

In this model, on this surface, the centrifugal force and airflow resistance of the particles are balanced:

$$\rho_t \frac{\pi d_t^3}{6} \frac{V_{\theta CS}^2}{0.5D} = 3\pi\mu d_t V_{rCS} \quad (3.1)$$

In the above formula, ρ_t is the density of plastic particles, d_t is the plastic particle diameter, $V_{\theta CS}$ is the tangential velocity of the particles on the CS surface, V_{rCS} is the axial velocity of the particles on the CS surface, and D is the diameter of the cyclone separator [14].

3.2 Theoretical Calculation of Separator

3.2.1 Calculation of separation efficiency

$$\eta = 1 - \exp\left\{-\frac{2R_Z^2}{R_Z^2 - R_W^2} \left[(m+1) \frac{\rho_p}{9\mu_g} \left(\frac{2\mu_{sz} d_p}{R_Z}\right)^2 t_p\right]^{\frac{1}{2m}}\right\} \quad (3.2)$$

Where:

$$t_p = \frac{V_s}{V}$$

$$V_s = \frac{\pi h_s (D_Z^2 - D_W^2)}{4}$$

$$U_{sz} = V_{IN} + u_p \frac{R_W}{R_Z} = V_{IN} + \frac{R_V^2}{F}$$

$$m = \frac{\ln\left[\frac{\left(\frac{R_Z}{R_W}\right)^n + \frac{u_p}{V_{IN}}}{1 + \frac{u_p R_W}{V_{IN} R_Z}}\right]}{\ln\left(\frac{R_Z}{R_W}\right)}$$

$$n = 1 - \left[1 - \frac{(39.4D_z)^{0.14}}{2.5}\right] \left(\frac{T}{294.44}\right)^{0.3}$$

Among them, ρ_p Is the particle density, kg/m^3 ; μ_g Is the gas viscosity, $\text{Pa}\cdot\text{s}$; d_p Is the particle diameter, m ; t_p Is the residence time of the gas in the separator, s ; V Is the gas processing flow rate, m^3/s ; V_s is the separation space volume, hour ; h_s is the effective separation height of the cylinder, m ; D_z Is the diameter of the cylinder, m ; D_w is the diameter of the exhaust pipe, m ; U_{sz} is the tangential velocity of the air flow in the separation chamber, m/s ; V_{IN} is the air inlet velocity, m/s ; U_p Is the linear velocity of the entrance edge, m/s ; ω_p Is the rotational angular velocity of the impeller, m/s ; m is the speed release coefficient, a dimensionless coefficient; n is the rotation index, and T is the absolute temperature of the air in the separator, K .

3.2.2 Pressure loss calculation

$$\Delta P = \frac{1}{2} \zeta_{IN} \rho_g V_{IN}^2 + \frac{R_{IN} A}{R_W \alpha^2} \frac{(A \frac{R_{IN} + 2\alpha}{R_W})}{(A + \frac{R_W}{R_{IN}} \alpha)^2} \rho_g \frac{V_{IN}^2}{2} + \frac{\rho_g u_p^2}{2} \left(1 - \frac{R_{IN}}{R_W}\right) + \zeta_B \rho_g \frac{V_B^2}{2} \quad (3.3)$$

Where:

$$A = \frac{\pi h_s R_W}{2 F_{IN}} \lambda_s$$

$$\lambda_{out} = 0.11 \left(\frac{\Delta}{D_{out}} + \frac{68}{Re_{out}} \right)^{0.25}$$

$$Re_{out} = \frac{\rho_g V_{out} D_D}{\mu_g}$$

$$\alpha = 1 - (0.54 - 0.153 \frac{F_W}{F_{IN}}) \left(\frac{b}{R_Z} \right)^{1/3}$$

Among them D_{out} Is the diameter of the gas outlet pipe, m ; L_{out} Is the length of the gas outlet pipe, m ; A is the damage coefficient of the separation section, which is determined by the following formula; λ_{out} Is the export friction damage coefficient; α Is the inlet shrinkage coefficient; b is the gas inlet width, m ; F_W 、 F_{IN} The cross-sectional area of the cylinder and the inlet pipe, m^2 ; ζ_{IN} For the pressure damage coefficient caused by the expansion of the inlet gas, this paper takes $\zeta_{IN} = 1$; λ_s Is the friction coefficient, in this article $\lambda_s = 0.02$; ζ_B Is the pressure loss coefficient caused by the impeller, $\zeta_B = 20$; V_B Is the fluid velocity between blades, m/s ; Δ For export roughness; ζ_K Is the local damage coefficient of the outlet pipe.

3.3 The Process of Parametric Design

3.3.1 User requirements

User content should include own data, output requirements, sample data, sample results, etc. Collect and sort out relevant technical data, estimate whether the requirements of users can be realized, sort out all the system tools and software that may need to be used, and briefly conceive the structure of the system.

3.3.2 Realization method

Sorting out the realization methods of relevant requirements in the design requires sorting out the parameter selection principles and calculation methods, sorting out the simplest and most

necessary input parameter data dictionary, and summarizing the drawing requirements of the graphics to be generated.

3.3.3 Generate a bitmap

If you need to generate graphics, you need to first generate a basic point map in the AutoCAD interactive drawing mode: if the graphics to be generated are mechanical design drawings, you should draw the point map according to the typical size, and mark the control points in the drawing.

3.3.4 Overall design

Sort out the "data structure", "data flow", and "system block diagram" that meet user requirements according to the above conditions and the naming rules of symbols in each function. The next thing to do is to sort out the "data dictionary", "block diagram" and "incoming interface rules between the entire systems" of each specific function from top to bottom, from rough to fine, batch by function.

3.3.5 Detailed design

Compile VBA source program according to the requirements of system block diagram and point bitmap. It is required to debug the paragraphs written in time, and solve the problems encountered immediately, and finally achieve the goal that the results in the paragraphs are completely correct.

3.3.6 Overall debugging

After the debugging of all the functional modules is completed, add the correct description of the argument table, and use the main control program to debug and adjust until it succeeds. Then exit AutoCAD, reload and run. Repeatedly, the results of multiple tests are still correct, indicating that the program can complete the user's requirements.

3.3.7 Compile and package

After all the debugging is qualified, compile the related program into a VBA package, and organize the source program and related technical data [15].

4 EXPERIMENTAL RESULTS AND ANALYSIS

Use the compiled program to optimize the cyclone separator, and carry out the following operations and experiments.

4.1 Parameter Changes

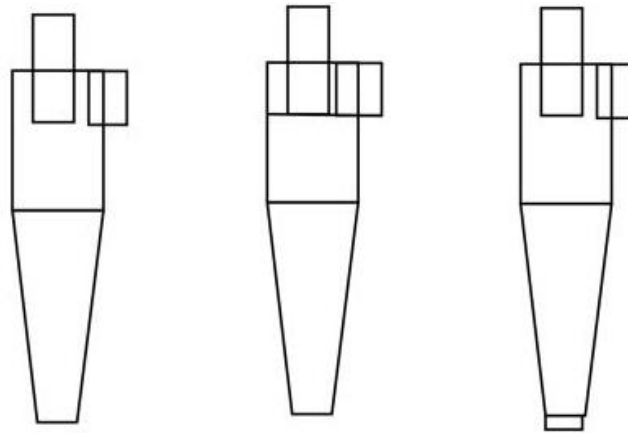
After analyzing the relationship between each factor and the response surface, the optimization goal is set, and the computer provides 3 candidate design points that meet the conditions according to theoretical predictions, of which the best design point is the inclination angle of the tapered pipe section $\alpha=5.7^\circ$, exhaust pipe insertion depth $s=809.3\text{mm}$ and exhaust pipe diameter $D_e=514.2\text{mm}$, the total separation efficiency is 91.3%; using the above structural parameters to calculate and verify the model, the actual total separation efficiency is 90.4 %, which is basically in line with the theoretical prediction value, which is 6.1% higher than the total separation efficiency of 84.3% before optimization, indicating that the method can truly reflect the influence of influencing factors on the separation efficiency of the cyclone separator. The changes of each parameter before and after model optimization are shown in Table 1.

Type	Tilt angle of conical tube	Exhaust pipe insertion depth (mm)	Exhaust pipe diameter (mm)	separation efficiency (%)	Static pressure drop (Pa)
------	----------------------------	-----------------------------------	----------------------------	---------------------------	---------------------------

Before optimization	6.2	787.0	472.0	84.3%	1198.3
Post optimality	5.7	809.0	514.2	90.4%	1263.8

Table 1: Parameter changes before and after optimization.

Figure 3 shows the geometric shape changes before and after optimization. The outer profile in Figure 3(c) is after optimization, and the interior is before optimization. It can be seen from Table 1 and Figure 3 that the geometry of the optimized cyclone has little change, the insertion depth of the exhaust pipe and the diameter of the exhaust pipe increase, the cone angle decreases, and the overall length becomes larger. The optimized shape is more optimized. The former is relatively slender, and such small changes in structural parameters are difficult to achieve with single-factor optimization.



(a) Before optimization (b) postoptimality (c) Geometric overlap

Figure 3: Shape comparison before and after optimization.

4.2 Pressure Drop Changes

The pressure drops before and after optimization obtained by FLUENT software is shown in Table 2. From Table 2, it can be seen that the static pressure drop, dynamic pressure drop and total pressure drop of the optimized cyclone separator are compared with those before optimization. Increase, but the amplitude of change is small, the difference is 65.5, 14.3, 50.4Pa, respectively, the energy consumption for gas-solid separation is basically the same.

Type	Static pressure drop	Dynamic pressure drop	overall pressure drop
Before optimization	1198.3	-172.4	9521
Post optimality	12638	-186.7	1002.5

Table 2: Pressure drop changes before and after optimization.

Figure 4 shows the static pressure drop cloud diagram before and after the optimization of the cyclone separator. It can be seen that the pressure distribution law before and after the optimization is inward along the radius, and the pressure gradually decreases until the pressure value at the central vortex approaches Zero; the central area presents a low pressure zone, extending to the exhaust port; the optimized pressure drop of the inner and outer swirling flow along the axial direction is greater than that before the optimization, and after the optimization, the air flow swing phenomenon at the tail of the optimized front cone section is weakened. It is consistent with the tangential velocity eccentricity, which prevents the back-mixing phenomenon of the quasi-forced vortex at the tail of the internal swirling flow, which is beneficial to the stability of the flow field, thereby improving the separation efficiency [16].

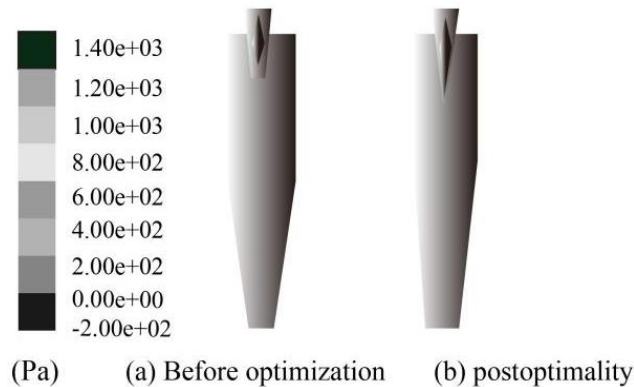


Figure 4: Cloud diagram of static pressure drop before and after cyclone separator optimization.

Figure 5 shows the static pressure distribution at X=3500mm before and after optimization. It can be seen that the pressure difference between the inside and outside of the gas phase increases after optimization, the pressure of the outer swirling flow is higher, and the pressure of the inner swirling flow is lower, which is conducive to promoting gas-solid separation.

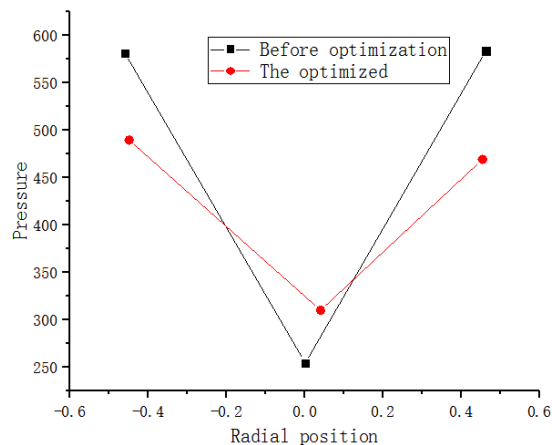


Figure 5: Static pressure distribution at X=3500mm before and after optimization.

Combining the speed and pressure drop changes, it can be seen that the increased tangential velocity due to the slender change of the cyclone geometry is converted from the increase in

pressure drop; the optimized pressure energy is reduced compared to before optimization, which complements the gas-solid separation. It requires kinetic energy and conforms to the law of conservation of energy. It is the conversion of this energy that improves the separation efficiency of the cyclone separator.

4.3 Changes in Separation Efficiency

The separation efficiency is an important indicator of the separation performance of the cyclone separator, which can be divided into total separation efficiency and fractionation efficiency. The above has carried out a comparative analysis on the total separation efficiency before and after optimization, and the total separation efficiency after optimization is significantly improved by 6.1% compared with that before optimization.

Some do not reach the bottom and directly into the exhaust pipe discharge, separation effect is poor. When the particles with particle size of 14 μ m run in the optimized cyclone separator, they will be thrown to the side wall due to a large centrifugal force, spiral down along the side wall, and discharged through the ash discharge port to achieve separation, with good separation effect.

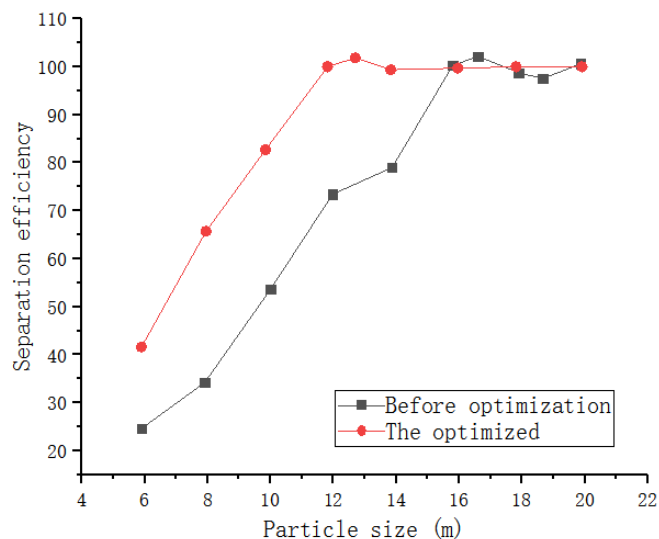


Figure 6: Comparison of separation efficiency before and after optimization.

Figure 6 shows the separation efficiency of the cyclone separator before and after the optimization. It can be seen that as the particle diameter increases, the separation efficiency of the cyclone separator gradually increases, and eventually stabilizes; under the same particle size conditions, the optimized separation efficiency before the complete separation is greater than that before the optimization; when the particle diameter is 16 μ m, the separation efficiency before optimization reaches 100%; when the particle diameter is 12 μ m, the optimized separation efficiency has reached 100%, which is due to optimization. Afterwards, the tangential velocity and velocity difference increase, which increases the centrifugal force of the particles, and the small particles are more easily thrown to the side wall to achieve separation. It can be seen that the separation performance of the optimized separator is stronger than that before the optimization, and it can complete the separation task of smaller particle size. This also shows that the fluid structure after the size optimization is optimized by the response surface method, and the separation efficiency is still can be further improved [17].

In order to meet the objective for performing an analysis and to calculate the pressure drop and efficiency of separation of cyclone separator model by changing the diameter of particle and velocity of particle individually.

Cyclone separation is a process of separating different phases of liquid for separating different particles from a stream of gas. In order to meet the objective, the authors have utilized a reverse flow cyclone separator as it is most commonly implemented these days.

The case studies carried out in order to check the performance of the system and below is the description of case 1.

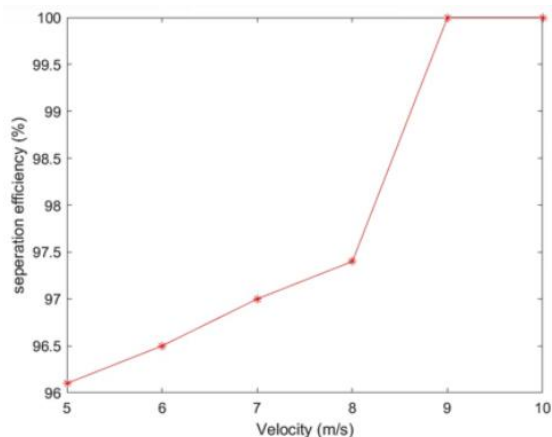
Case 1

The iteration count for case 1 is 550 and the system performance is evaluated for various particle and inlet velocity ranges from 5 m/s to 10 m/s.

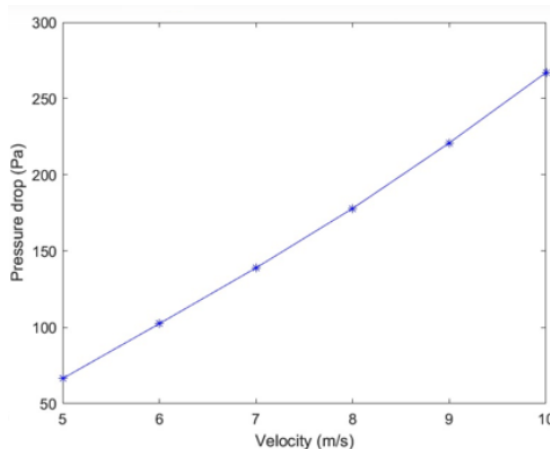
Table 3 represents the performance measurement 4 different particle and inlet velocities for trapped, tracked, escaped, pressure drop and the efficiency of separation.

Particle Velocity and Inlet Velocity	Trapped value	Tracked value	Escaped value	Pressure drop	Separation efficiency
5	242	235	8	65.4	0.951
6	242	236	7	101.3	0.953
7	242	237	6	138	0.96
8	242	238	5	176	0.97
9	242	243	0	220	1
10	242	243	0	266	1

Table 3: Pressure drop changes before and after optimization.



(a) Velocity vs efficiency



(b) Velocity vs pressure drop

Figure 7: (a) Percentage separation efficiency with respect to velocity, (b) Percentage pressure drop with respect to velocity.

Figure 7 (a) represents the graphical representation of percentage separation efficiency to the velocity and Figure 7 (b) represents the percentage pressure drop with respect to the velocity.

It is observed from the experimentation that the particle size is of great consideration as it effects the separators efficiency. The large amount of particles can be separated easily comparative to the smaller particles. With the increase in the velocity the efficiency of separation is also increased and with the increment in the inlet velocity the pressure drop in the system is increased.

5 CONCLUSION

In view of the problems encountered in the repetitive calculation of the cyclone separator and the drawing of parts and components encountered in the production of enterprises and factories, that is, the problems of more repetitive work and low work efficiency, it is developed based on VB and AutoCAD software. A set of parameterized design software system for the two-stage cyclone separator is taken. Take the inclination angle of the tapered pipe section, the exhaust pipe insertion depth s and the exhaust pipe diameter D , which have a significant effect on the separation efficiency. For design variables, with separation efficiency and pressure drop as objective functions, the structural parameters of the cyclone separator are optimized. The results show that the separation efficiency of the cyclone separator is increased from 84.3% to 90.4% by the response surface optimization method, and the speed, pressure drop, fractionation efficiency before and after optimization are compared and analyzed, and the optimization efficiency is found to be obvious.

Zhenhua Han, <https://orcid.org/0000-0002-4886-6271>

Mohammad Asif Iqbal, <https://orcid.org/0000-0001-6148-1555>

REFERENCES

- [1] Wang, B.; He, Z.; Song, L.; Chen, W.: Improved calculation of turbulence parameters based on six tropical cyclone cases: implication to wind turbine design in typhoon-prone areas, *Journal of Meteorological Research*, 33(5), 2019, 895-904. <https://doi.org/10.1007/s13351-019-8174-2>
- [2] Matros, E.; Albornoz, C.-R.; Rensberger, M.; Weimer, K.; Garfein, E.-S.: Computer-assisted design and computer-assisted modeling technique optimization and advantages over traditional methods of osseous flap reconstruction, *Journal of reconstructive microsurgery*, 30(05), 2014, 289-296. <https://doi.org/10.1055/s-0033-1358789>
- [3] May, L.-G.; Kelly, J.-R.; Bottino, M.-A.; & Hill, T.: Effects of cement thickness and bonding on the failure loads of CAD/CAM ceramic crowns: multi-physics FEA modeling and monotonic testing, *Dental Materials*, 28(8), 2012, e99-e109. <https://doi.org/10.1016/j.dental.2012.04.033>
- [4] Kim, J.; Pratt, M.-J.; Iyer, R.-G.; Sriram, R.-D.: Standardized data exchange of CAD models with design intent, *Computer-Aided Design*, 40(7), 2008, 760-777. <https://doi.org/10.1016/j.cad.2007.06.014>
- [5] Camba, J.-D.; Contero, M.; Company, P.: Parametric CAD modeling: An analysis of strategies for design reusability, *Computer-Aided Design*, 74, 2016, 18-31. <https://doi.org/10.1016/j.cad.2016.01.003>
- [6] Zhang, T.; Chakrabarty, K.; Fair, R.-B.: Behavioral modeling and performance evaluation of microelectrofluidics-based PCR systems using SystemC, *IEEE Transactions on Computer-Aided Design of Integrated Circuits and Systems*, 23(6), 2004, 843-858. <https://doi.org/10.1109/TCAD.2004.828115>
- [7] Jayanti, S.; Kalyanaraman, Y.; Iyer, N.; Ramani, K.: Developing an engineering shape

- benchmark for CAD models, *Computer-Aided Design*, 38(9), 2006, 939-953. <https://doi.org/10.1016/j.cad.2006.06.007>
- [8] Cheutet, V.; Daniel, M.; Hahmann, S.; La Greca, R.; Léon, J.-C.; Maculet, R.; Sauvage, B.: Constraint modeling for curves and surfaces in CAGD: A survey, *International Journal of Shape Modeling*, 13(02), 2007, 159-199. <https://doi.org/10.1142/S0218654307000993>
- [9] Brown, A.; Salcedo, J.: Multiple-objective optimization in naval ship design, *Naval Engineers Journal*, 115(4), 2003, 49-62. <https://doi.org/10.1111/j.1559-3584.2003.tb00242.x>
- [10] Chen, K.; Wang J.: Design of multivariate alarm systems based on online calculation of variational directions, *Chemical Engineering Research & Design: Transactions of the Institution of Chemical Engineers*, 2017. <https://doi.org/10.1016/j.cherd.2017.04.011>
- [11] Ometov, A.; Bezzateev, S.; Voloshina, N.; Masek, P.; Komarov, M.: Environmental monitoring with distributed mesh networks: An overview and practical implementation perspective for urban scenario, *Sensors*, 19(24), 2019, 5548. <https://doi.org/10.3390/s19245548>
- [12] Yeh, A.-C.; Tsao, T.-K.; Chang, Y.-J.; Chang, K.-C.; Yeh, J.-W.; Chiou, M.-S.; Murakami, H.: Developing new type of high temperature alloys-high entropy superalloys, *Int. J. Metall. Mater. Eng*, 1(107), 2015, 1-4. <https://doi.org/10.15344/2455-2372/2015/107>
- [13] Derevich, I.-V.; Panova, A.-A.: Calculation of the thermodynamic equilibrium of a multicomponent two-phase system based on minimization of the gibbs potential, *Journal of Engineering Physics and Thermophysics* (1), 2020. <https://doi.org/10.1007/s10891-020-02115-6>
- [14] Wang, J., Dagan, K. J., & Yuan, X., (2019). An Efficient Analytical Inductor Core Loss Calculation Method for Two-level and Three-level PWM Converters based on a User-friendly Loss Map. 2019 IEEE Applied Power Electronics Conference and Exposition (APEC). IEEE. <https://doi.org/10.1109/APEC.2019.8722114>
- [15] Sabah, F.; Wahid, A.; Nassih, F.; El Ghorba, M.; Chakir, H.: Prediction of the lifetime of acrylonitrile butadiene styrene (abs), by calculation of damage by two methods: damage based on residual stresses and damage by stages evolution, *Key Engineering Materials*, 2019, 820. <https://doi.org/10.4028/www.scientific.net/KEM.820.203>
- [16] Yuan, W.; Liu, M.; Wan, F.: Calculation of critical rainfall for small-watershed flash floods based on the hec-hms hydrological model, *Water Resources Management: An International Journal*, Published for the European Water Resources Association (EWRA), 2019. <https://doi.org/10.1007/s11269-019-02257-0>
- [17] Takaba, H.; Kimura, S.; Alam, M.-K.: Crystal and electronic structures of substituted halide perovskites based on density functional calculation and molecular dynamics, *Chemical Physics*, 485-486, 2017, 22-28. <https://doi.org/10.1016/j.chemphys.2016.12.007>